The use of the Master Curve in Structural Integrity Assessment

Kim Wallin [1, a]

[1] Academy of Finland, P.O.Box 1000, FI-02044 VTT,

[a] kim.wallin@vtt.fi

Keywords: Master Curve, Brittle fracture, Structural Integrity.

Abstract. The Master Curve (MC) methodology has evolved, from only being a brittle fracture testing and analysis procedure, to a technological tool capable of addressing many more structural integrity issues like constraint and parameter transferability. The MC enables a complete characterization of a material's brittle fracture toughness based on only a few small size specimens. The MC method has been shown to be applicable for practically all steels with a body-centered cubic lattice structure, generally identified as ferritic steels. The method has been described in detail in several publications. The method combines a theoretical description of the scatter, a statistical size effect and an empirically found temperature dependence of fracture toughness. The fracture toughness in the brittle fracture regime is thus described with only one parameter, the transition temperature T_0. The basic MC method has been standardized in the ASTM standard E1921, the first standard that accounts for the statistical specimen size effect and variability in brittle fracture toughness. In this presentation some of the more resent advances of the MC technology are highlighted, with special emphasis on problems related to the use of the Master Curve in Structural Integrity Assessment.

Introduction

Normally, fracture toughness testing standards require the use of comparatively large test specimens to obtain so called valid fracture resistance values. Extreme standards in this respect are the linear-elastic K_{IC} standard and the CTOD standard that require elastic behavior of the test specimen or full section thickness specimens, respectively. Often, like for operational structures, it is impossible or inappropriate to obtain large material samples for standard fracture toughness determination. This is especially the case with irradiation damage assessment of reactor pressure vessels, but also many other applications have the same restrictions. These specimen size requirements are a major obstacle for applying fracture mechanics in structural integrity assessment outside aviation, nuclear and off-shore industries.

At VTT, development work has been in progress for quarter of a century to develop and validate testing and analysis methods applicable for fracture resistance determination from small material samples. The VTT approach is a holistic approach by which to determine static, dynamic and crack arrest fracture toughness properties either directly or by correlations from small material samples. The Master Curve (MC) method is a statistical, theoretical, micromechanism based, analysis method for fracture toughness in the ductile to brittle transition region. The method, originally developed at VTT Manufacturing Technology" simultaneously account for the scatter, size effects and temperature dependence of fracture toughness [1].

The method has been successfully applied to a very large number of different ferritic steels and it forms the basis of the ASTM testing standard for fracture toughness testing in the transition region (ASTM E1921-02). Worldwide, there is ongoing comprehensive validation and development work to include the Master Curve method, as a new reference fracture toughness concept, into different structural integrity assessment codes, like ASME.

The MC enables a complete characterization of a material's brittle fracture toughness based on only a few small-size specimens. The MC method has been shown to be applicable for practically all steels with a body-centered cubic lattice structure, generally identified as ferritic steels. The fracture toughness in the brittle fracture regime is described with only one parameter, the transition temperature T_0. The basic form of the MC method is what has been standardized in the ASTM standard E1921.

The method enables the use of small specimens for quantitative fracture toughness estimation, thus reducing testing costs and enabling surveillance size specimens to be used for a direct measurement of fracture toughness. It also improves the quality of lower bound fracture toughness estimates, thus reducing the need for overly conservative safety factors. The applicability of the method is not restricted to nuclear applications. Its biggest impact is foreseen to be on fracture toughness determination for conventional structures, where testing costs and material use are presently inhibiting the use of fracture mechanics in design.

Recently, the MC methodology has evolved from only being a brittle fracture testing and analysis procedure to a technological tool capable of addressing many more structural integrity issues like constraint and parameter transferability.

The Basic Master Curve Method

The approach is based on a statistical brittle fracture model, which gives for the scatter of fracture toughness [2]:

$$P\left[K_{IC} \le K_I\right] = 1 - \exp\left(-\left[\frac{K_I - K_{min}}{K_0 - K_{min}}\right]^4\right) \tag{1}$$

where $P[K_{IC} \le K_I]$ is the cumulative failure probability, K_I is the stress intensity factor, K_{min} is the theoretical lower bound of fracture toughness and K_0 is a temperature and specimen size dependent normalization fracture toughness, that corresponds to a 63.2% cumulative failure probability being approximately $1.1 \cdot \overline{K}_{IC}$ (mean fracture toughness). The special form of Eq. 1 with $K_I - K_{min}$, instead of $K_I^4 - K_{min}^4$, comes from a conditional crack propagation criterion, which makes the MC to deviate from a simple weakest link model. The model predicts a statistical size effect of the form [2]:

$$K_{B_2} = K_{min} + \left[K_{B_1} - K_{min}\right] \cdot \left(\frac{B_1}{B_2}\right)^{1/4} \tag{2}$$

where B_1 and B_2 correspond to respective specimen thickness (length of crack front).

On the lower shelf of fracture toughness ($K_{IC} << 50$ MPa$\sqrt{m}$) the equations may be inaccurate. The model is based upon the assumption that brittle fracture is primarily initiation controlled, even though it contains the conditional crack propagation criterion. On the lower shelf, the initiation criterion is no longer dominant, but the fracture is completely propagation controlled. In this case there is no statistical size effect (Eq 2) and also the toughness distribution differs (not very much) from Eq 1. In the transition region, where the use of small specimens becomes valuable, however, Eqs 1 and 2 are valid.

For structural steels, a "Master Curve" describing the temperature dependence of fracture toughness is assumed [2]:

$$K_0 = 31 + 77 \cdot \exp\left(0.019 \cdot \left[T - T_0\right]\right) \tag{3}$$

where T_0 is the transition temperature (°C) where the mean fracture toughness, corresponding to a 25 mm thick specimen, is 100 MPa√m and K_0 is 108 MPa√m.

Eq 3 gives an approximate temperature dependence of the fracture toughness for ferritic structural steels and it is comparatively well verified. The term ferritic includes also quenched and tempered martensitic and bainitic structural steels. Keeping the temperature dependence fixed, decreases the effect of possible invalid fracture toughness values upon the transition temperature T_0. It should be remembered that Eq. 3 is empirical in nature and, even though ferritic steels generally seem to have similar temperature dependence, outlier behavior cannot be ruled out.

Effect of Constraint on the Master Curve

In a previous investigation, the Master Curve transition temperature T_0 has been connected to the specimen constraint, expressed in terms of the elastic T-stress [3]. The investigation indicated that there exists roughly a linear relationship between T_0 and T-stress. The proposed relation had the form given in Eq. 4 [3]:

$$T_0 \approx T_{0deep} + \frac{T_{stress}}{10\,\mathrm{MPa}/\mathrm{°C}} \quad : \text{for } T_{stress} < 0 \tag{4}$$

The relation was based on experimental behavior of fracture toughness measured with single edge notched bend specimens, SE(B), with varying crack lengths. At the time, it was commonly assumed that positive T-stress values would have only a minor effect on the fracture toughness. This has later been found not to be the case. Several studies reveal a significant difference between deeply cracked SE(B) and C(T) specimens, both of which show a positive T-stress [4].

The dependence described by Eq. 4 is based on an experimental investigation. As such, it must be regarded as being empirical in nature. However, a theoretical investigation based on the local approach, predict a similar trend as in Eq.4 (Gao and Dodds [5]). In that investigation, a three-parameter Weibull model was used in connection with a local approach analysis. The predicted constraint effect is function of both material strength properties as well as Weibull exponent m. Large values of the exponent m, predicts a larger constraint dependence than small values. In the classical two-parameter local approach, m values have been found to lie close to 20, but the use of a three-parameter model has a tendency to decrease m considerably. Eq. 4 is in line with the local approach predictions. The local approach analysis also indicates that a linear approximation between T-stress and T_0 is appropriate. When the results are expressed in the form of absolute T-stress values, the materials mechanical properties seems to have a surprisingly little effect on the constraint dependence.

Eq. 4 does have some limitations, it neglects effects of positive T-stress, it is based on a simplified linear-elastic analysis and it is only based on SE(B) specimen behavior. All these issues call for a more thorough investigation. The applicability of the simplified T-stress constraint description must be tested on other specimen geometries and it must be compared to the elastic-plastic Q-parameter. Furthermore, the validity of Eq. 4 must be compared against the proportional T-stress value, normalized with the yield strength.

Comparison between T-stress/σ_Y and Q. O'Dowd and Fong Shih [6] present elastic-plastic Q solutions for three common specimen geometries. These results were compared with the simple linear-elastic T-stress/σ_Y estimates. Fig. 1 shows as an example the comparison for an DEN(T) specimen. Regardless of crack length, the similarity between Q and T-stress/σ_Y is striking. Up to general yield, the estimates are within 10 % of the yield strength. This finding partly explains the success of the T-stress in describing the constraint effect. In the case of SE(B) and CC(T) specimens,

the compliance between T-stress and Q is even better than for the DEN(T) specimen [7]. Overall, the T-stress/σ_Y provides a satisfactory approximation of Q and the T-stress appears to be applicable also for other specimen geometries than SE(B).

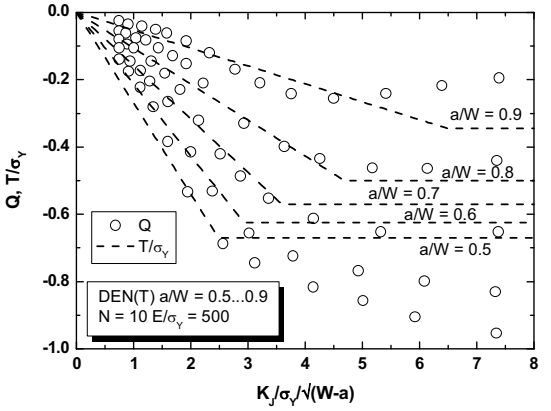

Figure 1. Comparison of development of T-stress and Q parameter as a function of loading for a DEN(T) specimen [6].

Verification of constraint effect for surface-cracked specimens. Fig. 2 [7] shows a verification of the constraint effect also for other specimens than SE(B). The surface cracked specimens are most realistic with respect to real structures and provide therefore a good validation of the overall applicability of the Master Curve also with realistic low-constraint geometries.

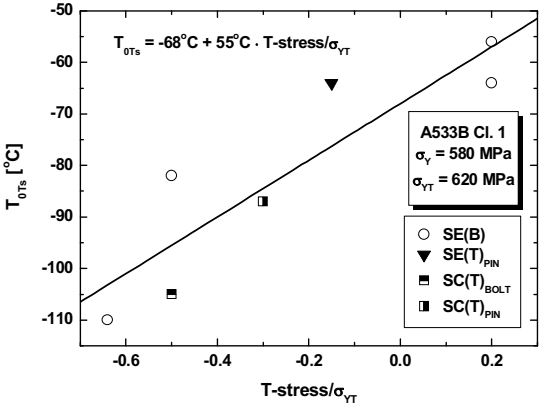

Figure 2. T-stress/σ_Y vs. T_0 dependencies including surface cracked specimens [7].

Validity of MC constraint adjustment. For the validation, a considerable number of materials and specimen test geometries were analyzed to examine the relation between the Master Curve T_0

transition temperature and the geometry related constraint expressed by the T-stress. In all cases, the relation between T_0 and T-stress could be satisfactorily approximated by a straight line relationship. The straight line approximation appears to be valid also for positive T-stress values of the magnitude encountered in the analysis (T-stress < 300 MPa). The functional form of the defined constraint dependence contained also the materials yield strength:

$$\Delta T_0 = A \cdot \frac{T-stress}{\sigma_{YT}} \tag{5}$$

The previously proposed relation did not contain the yield strength (Eq. 4). There are indications that yield strength may in reality play a rather small role in the constraint relation. This was studied in more detail by plotting the constant A as a function of the average yield strength of the materials. Only cases where the T-stress/σ_{YT} difference was more than 0.4 were included in the examination. A smaller difference would be unduly affected by the uncertainty in T_0 estimates. The plot is presented in Fig. 3 [7]. The yield strength has a significant effect on the constraint sensitivity. The higher the yield strength, the bigger the sensitivity is. The sensitivity is not related to material type, as seen by the similar behavior of A508 and A533B type steels. Actually, the yield strength effect may largely be apparent. The sensitivity is more likely affected by the strain hardening, but since the strain hardening and yield strength are related, yield strength appears to affect the sensitivity. An approximate average description of the sensitivity is represented by A = σ_{YT}/12 MPa/ºC which would lead to:

$$\Delta T_0 = \frac{T-stress}{12\ MPa/°C} \text{ (for T-stress < 300 MPa)} \tag{6}$$

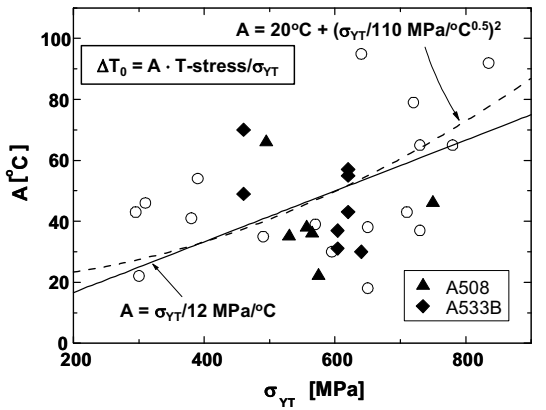

Figure. 3. Relation between constraint sensitivity (A) and yield strength (σ_{YT}) [7].

A slightly better fit is obtained by using a non-linear (or even bi-linear) dependence to describe the constraint sensitivity. From a engineering point of view, the assumed form for the dependence does not produce radically different results.

Eq. 6 differs slightly from the original relation (Eq. 4), but the equations differs in that Eq. 4 does not assume any constraint effects for positive T-stresses, whereas Eq. 6 do. Thus, this new finding does not invalidate the previous conclusions. The new result is just more accurate in that it also includes the effect of positive stresses.

The Warm Pre-Stress (WPS) effect and the Master Curve

The WPS effect describes the effect of a prior loading on the subsequent effective fracture toughness. When a crack is loaded to some fracture mechanical load level, which is lower than the fracture toughness at the temperature in question, the effect will be an effective increase in fracture toughness if the specimen is re-loaded at a lower temperature where the prior loading exceeds the fracture toughness (Fig. 4). The WPS does not affect the materials fracture toughness directly. It alters the stress field around the crack and this way produces an apparent increase of toughness. The WPS effect can be connected to a variety of possible transients, some of which are depicted in Fig. 4. Experimental investigations have focused on LCF (Load Cool Fracture), LUCF (Load Unload Cool Fracture) and LPUCF (Load Partial Unload Cool Fracture). A considerable amount of research, verifying the effect has been performed during the last 30 years [8]. The existence of the WPS effect is unquestionable if the result is not affected by time dependent processes like strain aging. Several investigations have shown that strain aging decreases, or even removes, the WPS effect [8]. The WPS effect is thus not recommendable for mitigation purposes, but in a structural integrity analysis, involving a prior overload or thermal transient, the effect can well be accounted for.

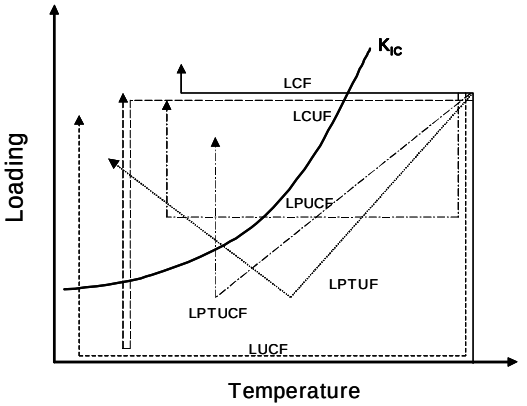

Figure 4. Principle of WPS effect [8].

In [8] a total of 751 WPS test results were collected from the literature. The majority of results (456) corresponded to the load-unload-cool-fracture (LUCF) transient. The second largest group (192) corresponded to the load-cool-fracture (LCF) transient. Smaller groups corresponded to the load-partial-unload-cool-fracture (LPUCF) with 18 results, the load-cool-unload-fracture (LCUF) with 17 results, the load-partial-transient-unload-fracture (LPTUF) with 8 results and the load-partial-transient-unload-cool-fracture (LPTUCF) with 60 results.

Based on the LCF and LUCF data a new simple WPS correction was developed:

$$
\begin{aligned}
&K_f = 0.15 \cdot K_{IC} + \sqrt{K_{IC} \cdot \left(K_{WPS} - K_2\right)} + K_2 \\
&\text{if} \quad K_2 \geq K_{WPS} - K_{IC} \Rightarrow K_2 = K_{WPS} \\
&\text{if} \quad K_f \leq K_{IC} \Rightarrow K_f = K_{IC}
\end{aligned}
\tag{7}
$$

In Eq. (7) K_2 is the "unloading" WPS value. If $K_2 \geq K_{WPS} - K_{IC}$ then K_2 gets the value of K_{WPS} and if $K_f \leq K_{IC}$ no WPS effect is present and K_f is equal to K_{IC}.

The new simple WPS correction has been shown to provide equal accuracy for all different WPS transients, making it thus generally applicable. In order to find out, if a yield stress change correction

really is needed for the simple method, the LCF data, where the yield stress effect should be most straightforwardly visible, was examined further. The effects of yield strength changes, on the WPS effect, during the transient, were found not to be statistically significant. The multiplication constant in Eq. 7 was taken as 0.15 as to provide a slight built-in conservatism of the correction (A best fit would yield a constant of 0.25).

Besides simplicity, the WPS correction also provides a consistent lower bound failure value if a lower bound fracture toughness value is used as input. The lower bound nature of the MC fracture toughness estimates also remain after the WPS correction. The new simple WPS correction is thus capable of handling any WPS transient with satisfactory accuracy and, combined with the Master Curve, is also capable to handle the effect of WPS on the apparent fracture toughness scatter, enabling the estimation of desired lower bound values.

Transferability of the Master Curve to Structures

Normally, the Master Curve parameters are determined using test specimens with "straight" crack fronts and comparatively uniform stress state along the crack front. This enables the use of a single K_I value and single constraint value to describe the whole specimen. For a real crack in a structure, this is usually not the case. Normally, both K_I and constraint varies along the crack front and in the case of a thermal shock, even the temperature will vary along the crack front. Generally real cracks are simplified in the form of ellipses in order to aid the analysis. For a real three dimensional crack, both K_I and K_0 may vary as a function of angular location (Φ) along the crack front. This leads to the need of a more general expression for the cumulative failure probability, than represented by the basic MC Eq. 1. A possible form is given by Eq. 8 [9]. The expression gives the cumulative failure probability, but it is not suited for a simple visualization of the result.

$$P_f = 1 - \exp\left\{\int_0^s \left(\frac{K_{I\Phi} - K_{min}}{K_{0\Phi} - K_{min}}\right)^4 \cdot \frac{ds}{B_0}\right\} \tag{8}$$

A visualization, that is in line with present structural integrity practice, can be achieved by defining an effective stress intensity factor K_{Ieff} corresponding to a specific reference temperature. The reference temperature can, for example, be chosen as the minimum temperature along the crack front. The procedure is to determine an effective driving force, which would give the same failure probability as Eq. 1, in the context of a standard Master Curve presentation. This means essentially a combination of Eqs. 1 and 8. The result is presented in Eq. 9 [9].

$$K_{IeffTref} = \left\{\int_0^s \left(\frac{K_{I\Phi} - K_{min}}{K_{0\Phi} - K_{min}}\right)^4 \cdot \frac{ds}{B_0}\right\}^{1/4} \cdot \left(K_{0Tref} - K_{min}\right) + K_{min} \tag{9}$$

$K_{I\Phi}$ is obtained from the stress analysis as a function of location (Φ. K_{0Tref} is the standard, high constraint, Master Curve K_0, corresponding to a reference temperature along the crack front and it has the form:

$$K_{0Tref} = 31 + 77 \cdot \exp\left[0.019 \cdot \left(T_{ref} - T_0\right)\right] \tag{10}$$

$K_{0\Phi}$ is the local K_0 value, based on local temperature and constraint. It can be expressed based on Eqs. 4 or 6 and has in the latter case the form:

$$K_{0\Phi} = K_{0T,T-stress} = 31 + 77 \cdot \exp\left[0.019 \cdot \left(T - T_{0,T-stress=0} - \frac{T - stress}{12MPa/°C}\right)\right] \quad (11)$$

The difference to the presently used visualization is that the fracture toughness is not directly compared to the crack driving force estimated from stress analysis. Instead, the fracture toughness is compared to an effective driving force, which accounts for the local stress and constraint state and temperature along the crack front, as well as the crack front length. This way it is possible to combine the classical way of fracture mechanical analysis and state of the art Master Curve analysis, and presenting the analysis result in a conventional format.

The one thing to remember, however, is that postulated flaws often contain unrealistically long crack fronts. A quarter thickness size flaw assumption may be justified, purely from a driving force perspective (as originally has been the intention). From a statistical size adjustment point of view, the assumption is over-conservative. If such postulated flaws are analyzed using K_{Ieff}, an additional size adjustment is recommended. A more realistic maximum crack front length for postulated flaws is 150 mm. This value is also in line with the original K_{IC} data used to develop the ASME K_{IC} reference curve and therefore justifiable in terms of the functional equivalence principle.

Inhomogeneous Master Curve

Recently, new MC analysis algorithms have been developed for the analysis of inhomogeneous data sets [10]. The algorithms are applicable both for bimodal inhomogeneities as well as random inhomogeneities [10]. The bimodal Master Curve algorithm is especially intended for the analysis of heat affected zone (HAZ) fracture toughness results, which are known to consist of a ductile and brittle constituent. With the new algorithm it may be possible to omit the requirement of making metallurgical sectioning of HAZ test specimens subsequent to testing. The randomly inhomogeneous Master Curve algorithm is mostly intended for the analysis of pooled data sets or materials with macroscopic segregations etc.

Bimodal Master Curve. In the case when the data population of a material consists of two combined MC distributions, the total cumulative probability distribution can be expressed as a bimodal distribution of the form:

$$P_f = 1 - p_a \cdot \exp\left\{-\left(\frac{K_{JC} - K_{min}}{K_{01} - K_{min}}\right)^4\right\} - (1 - p_a) \cdot \exp\left\{-\left(\frac{K_{JC} - K_{min}}{K_{02} - K_{min}}\right)^4\right\} \quad (12)$$

where K_{01} and K_{02} are the characteristic toughness values for the two constituents and p_a is the probability of the toughness belonging to distribution 1. In the case of multi-temperature data, the characteristic toughness (K_{01} and K_{02}) is expressed in terms of the MC transition temperature (T_{01} and T_{02}). In contrast to a standard MC analysis, where only one parameter needs to be determined, the bimodal distribution contains three parameters. This means that the fitting algorithm is somewhat more complicated than in the case of the standard MC. In order to be able to handle randomly censored multi-temperature data sets, the estimation must be based on the maximum likelihood procedure.

The likelihood is expressed as:

$$L = \prod_{i=1}^{n} f_{ci}^{\delta_i} \cdot S_{ci}^{1-\delta_i} \quad (13)$$

where f_c is the probability density function, S_c is the survival function and δ is the censoring parameter.

The probability density function and the survival function are respectively:

$$f_c = 4 \cdot p_a \cdot \frac{(K_{JC} - K_{min})^3}{(K_{01} - K_{min})^4} \exp\left\{-\left(\frac{K_{JC} - K_{min}}{K_{01} - K_{min}}\right)^4\right\} + 4 \cdot (1 - p_a) \cdot \frac{(K_{JC} - K_{min})^3}{(K_{02} - K_{min})^4} \cdot \exp\left\{-\left(\frac{K_{JC} - K_{min}}{K_{02} - K_{min}}\right)^4\right\} \quad (14)$$

$$S_c = p_a \cdot \exp\left\{-\left(\frac{K_{JC} - K_{min}}{K_{01} - K_{min}}\right)^4\right\} + (1 - p_a) \cdot \exp\left\{-\left(\frac{K_{JC} - K_{min}}{K_{02} - K_{min}}\right)^4\right\} \quad (15)$$

The parameters are solved so as to maximize the likelihood given by Eq. 13. The numerical iterative process is simplified by taking the logarithm of the likelihood so that a summation equation is obtained (Eq. 16).

$$\ln L = \sum_{i=1}^{n} \left[\delta_i \cdot \ln(f_{ci}) + (1 - \delta_i) \cdot \ln(S_{ci})\right] \quad (16)$$

The standard deviation of T_0 for the more brittle material can be approximated by Eq. 17, the more ductile material by Eq. 18 and the uncertainty of the occurrence probability of the more brittle material by Eq. 19.

$$\sigma T_{01} \approx \frac{22°C}{\sqrt{n \cdot p_a - 2}} \quad (17)$$

$$\sigma T_{02} \approx \frac{16°C}{\sqrt{r - n \cdot p_a - 2}} \quad (18)$$

$$\sigma p_a \approx \frac{0.35}{\sqrt{n \cdot p_a - 2}} \quad (19)$$

In the equations, n is the total number of results and r is the number of non-censored results. If in any of the equations, the denominator becomes less than 1, the bimodal estimate of the parameter in question should not be used. The minimum data set size to be used with the bimodal distribution is approximately 12-15, but preferably the size should be in excess of 20. Eqs. 17-19 can also be used to judge the likelihood that the data represents an inhomogeneous material. A simple criterion can be expressed as:

$$|T_{01} - T_{02}| > 2 \cdot \sqrt{\sigma T_{01}^2 + \sigma T_{02}^2} \quad (20)$$

If the criterion in Eq. 20 is fulfilled, the material is likely to be significantly inhomogeneous. On the other hand a criterion for a homogeneous material can equally well be expressed as:

$$|T_{01} - T_{02}| < 0.5 \cdot \sqrt{\sigma T_{01}^2 + \sigma T_{02}^2} \quad (21)$$

If the criterion in Eq. 21 is fulfilled, the material is likely to be homogeneous.

Master Curve Analysis of Random Inhomogeneities. The random variable T_0 is assumed to follow a Gaussian distribution characterized by mean T_{0MML} and standard deviation σT_{0MML}. The probability density function for T_0 is in this case:

$$f_T = \frac{1}{\sigma T_{0MML} \cdot \sqrt{2\pi}} \cdot \exp\left\{ -\frac{\left(T_0 - T_{0MML}\right)^2}{2 \cdot \sigma T_{0MML}^2} \right\} \tag{22}$$

The conditional survival probability at T_0 is the standard MC expression:

$$S_{T0} = \exp\left\{ -\left(\frac{K_{JC} - K_{min}}{K_0 - K_{min}} \right)^4 \right\} \tag{23}$$

where K_0 is dependent on T and T_0 according to the standard Master Curve.

The local conditional density probability at T_0 becomes accordingly:

$$f_{T0} = 4 \cdot \frac{\left(K_{JC} - K_{min}\right)^3}{\left(K_0 - K_{min}\right)^4} \cdot \exp\left\{ -\left(\frac{K_{JC} - K_{min}}{K_0 - K_{min}} \right)^4 \right\} \tag{24}$$

The total survival probability S is obtained by solving the integral:

$$S = \int_{-\infty}^{\infty} f_T \cdot S_{T0} \cdot dT_0 \tag{25}$$

and the corresponding total distribution function is:

$$f = \int_{-\infty}^{\infty} f_T \cdot f_{T0} \cdot dT_0 \tag{26}$$

The parameters T_{0MML} and σT_{0MML} are then solved by maximizing Eq. 16, using Eqs. 25 and 26 as input parameters.

A simple criterion to judge the likelihood that the data represents an inhomogeneous material is given by:

$$\sigma T_{0MML} > 2 \cdot \sigma T_{0E1921} \tag{27}$$

I.e. the steel is likely to be significantly inhomogeneous if the standard deviation from the MML estimate is bigger than twice the theoretical uncertainty in T_0 for a homogeneous steel.

A simple criterion to judge the likelihood that the data represents a homogeneous material is given by:

$$\sigma T_{0MML} < 0.5 \cdot \sigma T_{0E1921} \tag{28}$$

I.e. the steel is likely to be fully homogeneous if the standard deviation from the MML estimate is less than half the theoretical uncertainty in T_0 for a homogeneous steel.

Acknowledgements

This work is part of the authors Academy Professorship and is funded by the Academy of Finland decision 117700.

References

[1] K. Wallin: Int. J. of Materials and Product Technology Vol. 14, (1999), p. 342.

[2] K. Wallin: Journal de Physique IV, Colloque C7, supplément au Journal de Physique III Vol. 3, (1993), p. 575.

[3] K. Wallin: Engng. Fract. Mech. Vol. 68, (2001), p. 303.

[4] K. Wallin, T. Planman, M. Valo and R. Rintamaa: Engng. Fract. Mech. Vol. 68, (2001), p. 1265.

[5] X. Gao and R.H. Jr. Dodds: Engng. Frac. Mech. Vol. 68, (2001), p. 263.

[6] N.P. O'Dowd and C. Fong Shih: ASTM STP 1207, (1994), p. 21.

[7] K. Wallin, in: *Engineering Structural Integrity: resarch, development and application, ESIA9*, edited by S. J. Wu, P. E. J. Flewitt, B. Tomkins, Z. Zhang, J. Sharples, H. Y. Luo, EMAS Publishing Vol. 1 (2007), p. 149.

[8] K. Wallin: Engng. Fract. Mech. Vol. 70, (2003), p. 2587.

[9] K. Wallin: Nucl. Engng. and Design Vol. 237, (2007), p. 1388.

[10] K. Wallin, P. Nevasmaa, A. Laukkanen and T. Planman: Engng. Fract. Mech. Vol. 71, (2004), p. 2329.